

TRIBOLOGY RESEARCH OF THE TURNED ZIRCONIUM-DIOXIDE CERAMICS

Gellért Fledrich, Róbert Keresztes, László Zsidai

Institute for Mechanical Engineering Technology,
Faculty of Mechanical Engineering, Szent István University, Gödöllő, Hungary
www.geti.gek.szie.hu

Abstract The zirconium dioxide as basic material is suitable to machine by tool with regular edge deriving from lower ceramic hardness and from other characteristics so in case of piece production or small – and medium series production, at quick prototype production can become potential material alike. The aims to compare the arising frictional characteristics in case of dry friction condition in case of ceramic – steel surface pairs machined with different sets. We have developed for an equipment to carry out tribological tests. During the test we pressure the steel counter face with determined normal direction force the casing surface of the rotating ceramic specimen and in the meantime we measure the value of the friction force with force meter cell. We have calculated the friction coefficient characterizing the system from the normal direction force and the friction force as well as we measured the wear of the steel specimen and its deformation.

Keywords: ceramic, zirconium dioxide, tribo test, friction, wear, turning

1 INTRODUCTION

Important research results were achieved in the domain of zirconium-dioxide in nineteen eighties by HEVER and his fellow 1981; CLAUSSEN and his fellows 1983; SOMIYA and his fellows 1986; STEVENS 1986; HEVER 1987. The literature sources don't refer to the turning machining concerning ceramics, thus zirconium dioxide and aluminium oxide. Nowadays the grinding is the machining after the generally wide-spread sintering. The development of the finished- and semi finished products' manufacturing requires cutting ever more complex surfaces. The more economical machining of 3D surface requires the further development of tools with regular edge. Beside this application of ceramics spreads to the field of sliding bearings in engineering practice nowadays, too. Sliding bearing bushes are manufactured often and they are used in different places, it would be advantageous producing them by machining (for example: shape- and dimension accuracy). The operation of sliding bearings can be imagine in both dry conditions or in pump cases supplied with water lubrication. We have carried out tribological tests on ceramic surfaces grinded originally and on surfaces machined with different cutting parameters, steel counter surfaces were used.

2 TESTING METHODS, INSTRUMENTS

2.1 Materials tested

During machining from the two tool materials the material machined by polycrystal diamond proved to be appropriate. Because of this we have carried out the frictional tests on specimens cut by PCD-tool and on surfaces grinded originally. Figure 1. shows the frictional paths on the ceramic surface after test as well as the worn steel-plate can be seen.



Figure 1. Frictional path formed on the ceramic surface and a worn steel specimen.

Zirconium-dioxide ceramic specimen

The characteristics of the ZN 40 engineering ceramic is that it has got favourable physical and chemical characteristics at high temperature range. It has got high hardness (1250 HV), because of this it can be cut only with polycrystal diamond and with cubic boron nitride tools. The material tested is a zirconium dioxide ceramic stabilized with magnesium. The diameter of the cylindrical specimens was 16 mm used at tests.

We have machined the surface of ceramic with different settings. Based on preliminary measuring we established that it is expedient to choose the depth of cut between 0,01 and 0,05 mm, the feed rate should be between 0,01 and 0,05 mm/rev. immediately at the tool edge. We also carried out preliminary measuring concerning the approximate value of the cutting speed, this was around 50 m/min.

Steel specimen

To measure the frictional force we placed steel specimen to the ceramic surface. The material of the steel plates was St37F dimension 20x20 mm, thickness 1,5 mm. The contact surface was grinded, its average surface roughness was: $R_a=0,8$.

2.2 Equipment used for tests

Figure 2. shows the arrangement sketch of our testing equipment. We made new specimen holders and a drive to the basic equipment published earlier (Zsidai et al, 2006; Lefánti et al 2011) this can be seen in Figure 3.

The test principle is the so called *Block on Ring*, we pressed the steel counter-surface to the surface of the rotating ceramic specimen, and in the meantime we measured the friction force with a force meter cell. We calculated the friction coefficient characterizing the system from the normal direction pressing force and from the friction force, as well as we measured the wear and deformation (dimension change in vertical position, expressed in mm) of the steel specimen. We completed the ceramic clamping mandrel to the driving motor shaft on the equipment. We clamped the ceramic specimen to this. We pressed the grinded steel counter-surface with screw to the end of the force meter cell placed over the ceramic specimen. We adjusted the load with sliding masses on the road. The peripheral speed can be changed by the motor's number of revolution rotating the ceramic.

The measuring system models dry friction, separate lubrication was not used. We cleaned the surfaces on each other with denaturated alcohol before measuring.

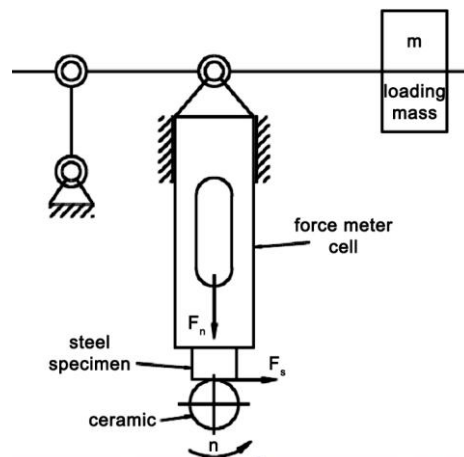


Figure 2. The theoretical sketch of the equipment testing the friction



Figure 3. The basic equipment (Zsidai et al 2006; Lefánti et al 2011) and the clamped ceramic and steel specimens developed to the frictional test.

2.3 The relation of the contact (Hertz) stress

We have determined the relation of the contact (Hertz) stress applied at the connection between cylinder-plane contact shown in Figure 4.

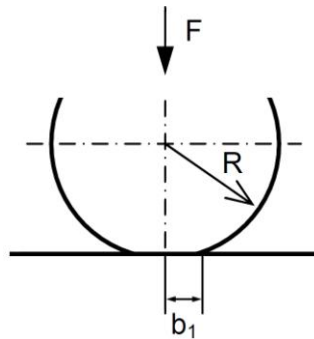


Figure 4. Cylinder-plane model (Van Beek, 2006)

The greatest value of the contact stress concerning the cylinder-plane contact according to Hertz-theory (Van Beek, 2006):

$$\sigma_{\max} = \frac{4}{\pi} \cdot p_m = \frac{4}{\pi} \cdot \frac{F}{A} = \frac{4}{\pi} \cdot \frac{F}{2 \cdot b_1 \cdot l} = \frac{2 \cdot F}{\pi \cdot b_1 \cdot l} \quad [\text{N/mm}^2] \quad (1)$$

where: p_m – is the average contact pressure (N/mm²)

F – is the loading force (N)

A – is the contact surface (mm²)

l – is the length of the contact surface (mm)

b_1 – is the half width of the contact surface (mm)

Based on Hertz's calculations the half width of the contact surface:

$$b_1 = \sqrt{\frac{8 \cdot F \cdot R}{\pi \cdot E' \cdot l}} \quad [\text{mm}] \quad (2)$$

where: R – is the radius of curvature (mm)

E' – is the equivalent elastic modulus (Mpa)

The equivalent elastic modulus (E'):

$$\frac{1}{E'} = \frac{1 - \nu_1^2}{2 \cdot E_1} + \frac{1 - \nu_2^2}{2 \cdot E_2} \quad [1/\text{MPa}] \quad (3)$$

where: ν_1 – is the Poisson's factor of the ceramic specimen

E_1 – is the elastic limit of the ceramic specimen (MPa)

ν_2 – is the Poisson's factor of the steel specimen

E_2 – is the elastic modulus of the steel specimen (MPa)

We have summed up the calculated Hertz-stress at the contact of ceramic-steel specimens used in the tests in Table 1. The following parameters were taken into account for the calculations:

ceramic: $E_1=210$ GPa, $\nu_1=0,3$

steel: $E_2=210$ GPa, $\nu_1=0,3$

radius: $R=8$ mm

load: $F=50$ N

test speed: $v_k=0,23$ m/s

Table 1. The calculated values

Equivalent elastic modulus (E') [MPa]	Half width of the contact surface (b_1) [mm]	Maximum contact stress according to Hertz (σ_{max}) [MPa]
230769	0,054	391,2

During test surface load developed from the linear load with the increasing of wear in the initial moment.

2.4 Parameters of the frictional tests

We have taken into account the conditions of engineering practical applications at the parameters set. The ceramic sliding bearings sliding speed is 1-5m/s at between general conditions. The diameter of the ceramic specimens was 16 mm, the width of the steel counter-piece was 1,5 mm. The linear contact is given from the contact geometry where we determined the value of the Hertz-stress taking into account the strength and geometric data, too.

Characters set:

sliding speed, v_k [m/s]

load, F_n [N]

Measured characters:

friction force, F_s [N]

wear, w [mm]

Calculated characters:

friction coefficient:

$$\mu = \frac{F_s}{F_n} \quad (4)$$

- F_s , friction force [N]

- F_n , normal direction force [N]

3 TEST RESULTS AND THEIR EVALUATIONS

3.1 "Basic" tests on the surfaces of grinded ceramic/steel

Figure 5. shows a measuring diagram of a friction force in the function of time. We changed the load in 3 steps. The initial load is 50 N (this corresponds with 391 MPa maximum Hertz-stress at linear contact). We started the measuring on this load, then after 5min. we increased the load to 100N. Again we increased the load to 150N after 5min. The test was continued on this level until the two surfaces were seized totally and the motor couldn't drive the mechanism. This happened at putting the greatest load in most cases. We marked the different loading sections on the diagram.

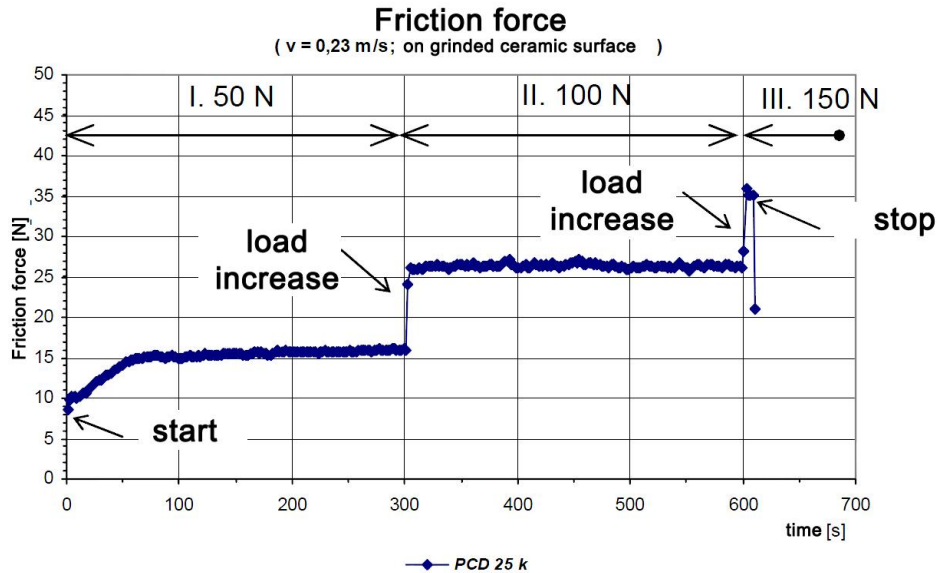


Figure 5. Friction force diagram (between steel/grinded ceramic surfaced)

The friction force settles after the running up at the beginning of the first section, and the friction force also increases at increasing the load. After 150N load the friction force increased so much that the motor stopped. This means the end of the measuring. Figure 6. Shows the measuring diagram of the wear and deformation in the function of time connecting with previous figure.

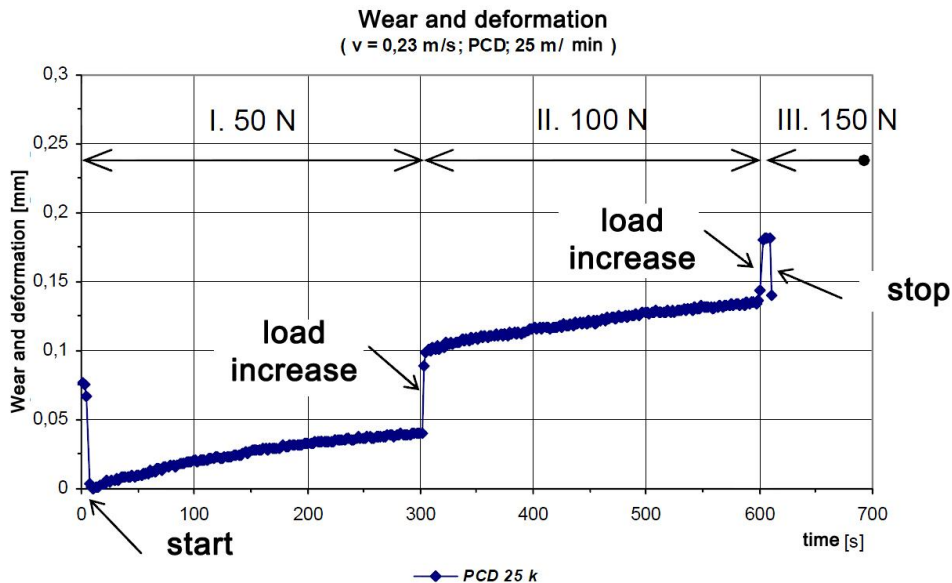


Figure 6. Wear and deformation diagram (between steel/grinded ceramic surfaces)

At increasing the load it can be seen in the diagram that the wear and deformation changed significantly. The size of the contact surface also changed with the increase of wear. The 391 MPa Hertz-stress calculated from the initial, linear contact decreases gradually within the loading sections.

We interpreted as a quotient of the vertical normal direction load and horizontal friction force the dry friction coefficient (μ) rising between the machined ceramic and steel surfaces. Figure 7. shows its change during the time of test. The loading section can also be separated well in this figure. By increasing the load the value of the friction coefficient decreased. The effect of the increase of wear, that is the increase of the contact surface are not significant concerning the change of the friction coefficient only at the beginning of the first section, when the linear contact transforms into surface contact. The value of

friction coefficient increases continuously in this running-in section. The effect of the surface increase to the value of the friction coefficient can't be indicated within the second section.

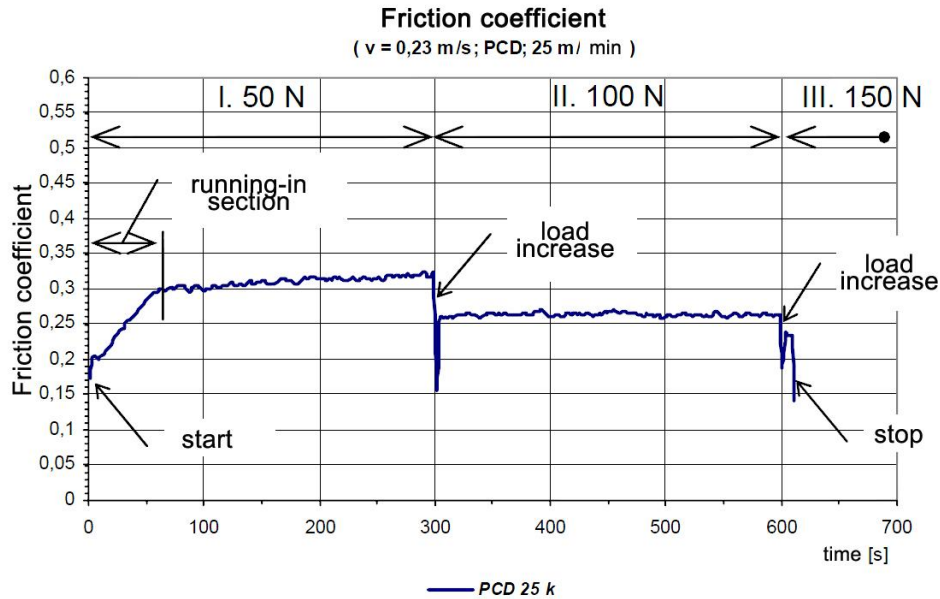


Figure 7. Friction coefficient diagram (between steel/ grinded ceramic surfaces)

3.2 Results of friction ($v_c = 25 \text{ m/min}$) and wear and their evaluation

We analysed in the followings the values of the friction coefficient, wear and deformation got in the friction model testing system produced during our research work. The polycrystal diamond tool material proved to be suitable from the two tool materials used during machining ceramic. Because of this we have carried out the frictional tests with the specimens cut with PCD tool as well as with the original surfaces grinded. On the casing surface of ZrO_2 ceramic tested at $v_c=25 \text{ m/min}$. cutting speed and 5 different feed rate ($f=0,01;-0,02;-0,03;-0,04;-0,05 \text{ mm/rev.}$) machined surface can be found. The width of these are 3 mm one by one. Figure 8. shows the value of arising friction force developed between the ceramic and the steel specimen, while the Fig. 9. shows the volume of wear and deformation. We distinguished the different surfaces with various colours and marks. The “k” marks the grinded surface (like Fig. 5, 6 and 7) while the numbers “1, 2, 3, 4, 5” mark the feed rates set during turning in hundredth millimetre.

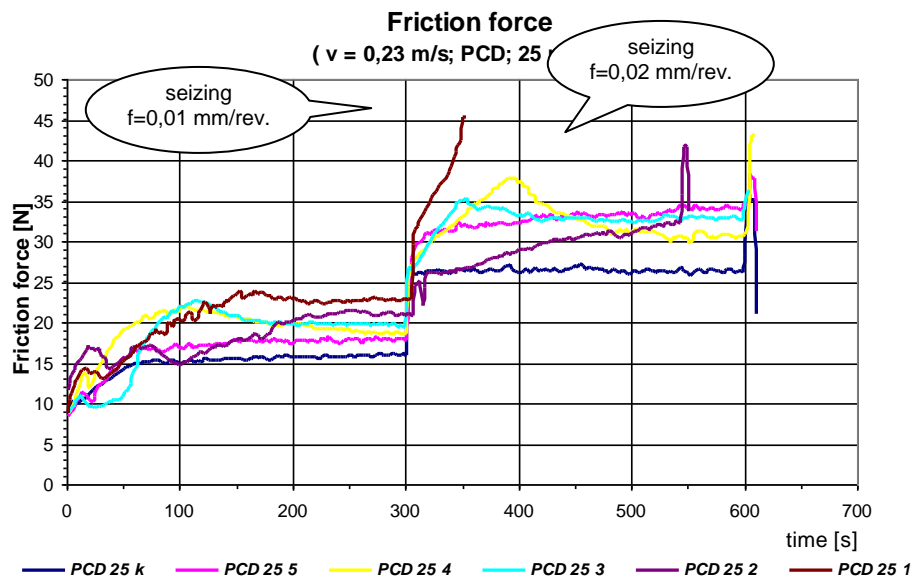


Figure 8. Friction force diagram (between steel/grinded and ceramic surface cut)

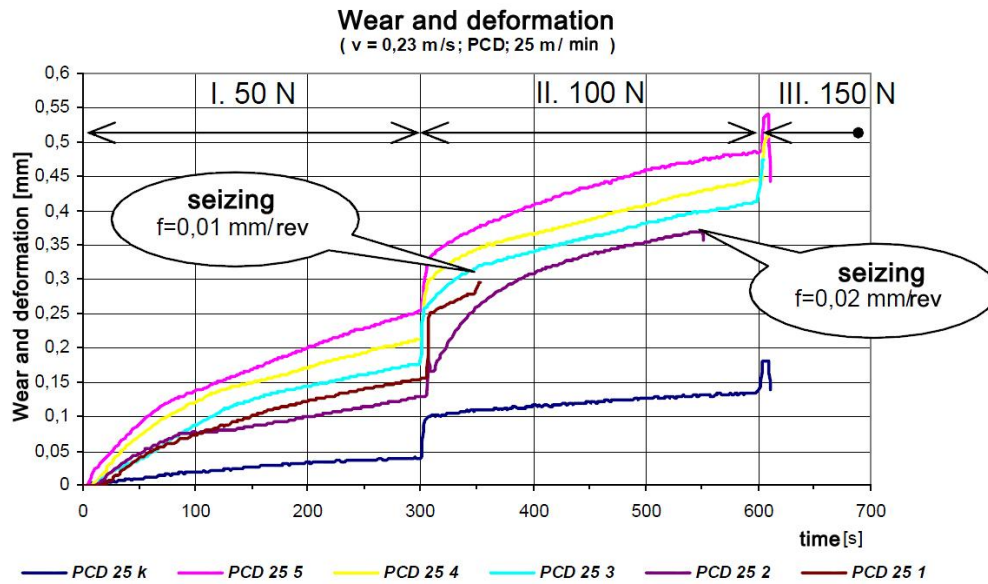


Figure 9. Wear and deformation time-diagram (between steel/grinded and turned ceramic surfaces)

The friction force didn't show significant change on the surface grinded within identical load section. It set in a nearly constant value within short time (50s). This can be explained these are few shell-like pitting on the ceramic surface and for lack of these the material pilling-of from the steel counter surface can't stick by this can't increase the friction force. The grinded surfaces also seized with imposing maximum load. It is striking on the diagram that the friction force increased in such a great extent on the 2. load level on the ceramic surfaces cut with 0,01 and 0,02 mm/re. feed rate, that the surfaces seized in this section. The seizing ensued on the 3. load level on surfaces cut with greater feed rate.

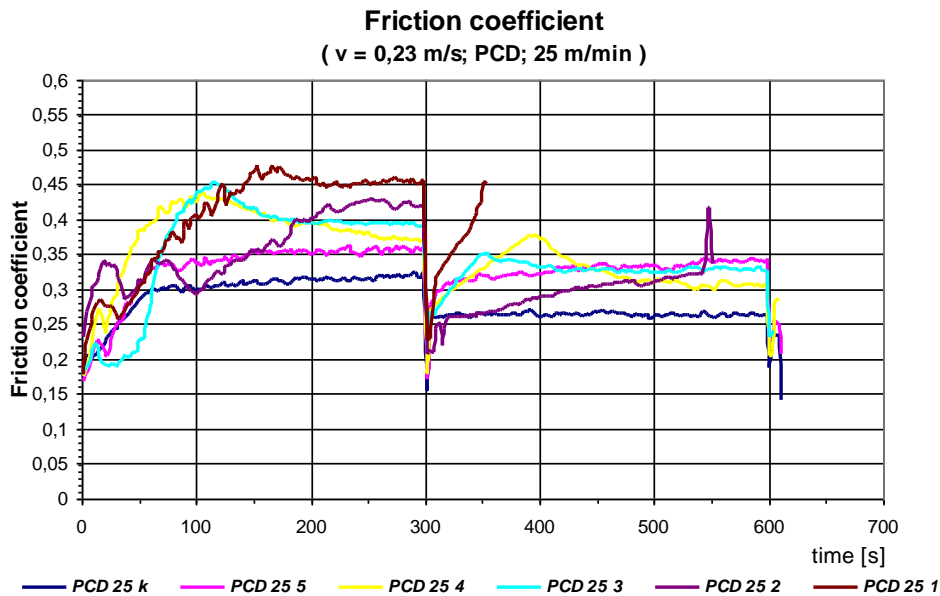


Figure 10. Diagram of friction coefficient (between steel/grinded and ceramic surface cut)

It is evident from the values of friction coefficients (Figure 10) that higher μ values characterize the surfaces machined with smaller feed rate. The value of friction coefficient on the surface turned with $f=0,05$ mm/rev. feed rate remained at nearly constant value in the sections tested similar to the grinded surface. Fluctuating friction coefficient, characterizing seizure can't be observed.

3.3 Results of friction ($v_c = 75 \text{ m/min}$) and wear and their evaluation

We make it known the measuring values of the friction as well as the wear and deformation carried out at 75m/min. cutting speed on the machined ceramic case in the followings.

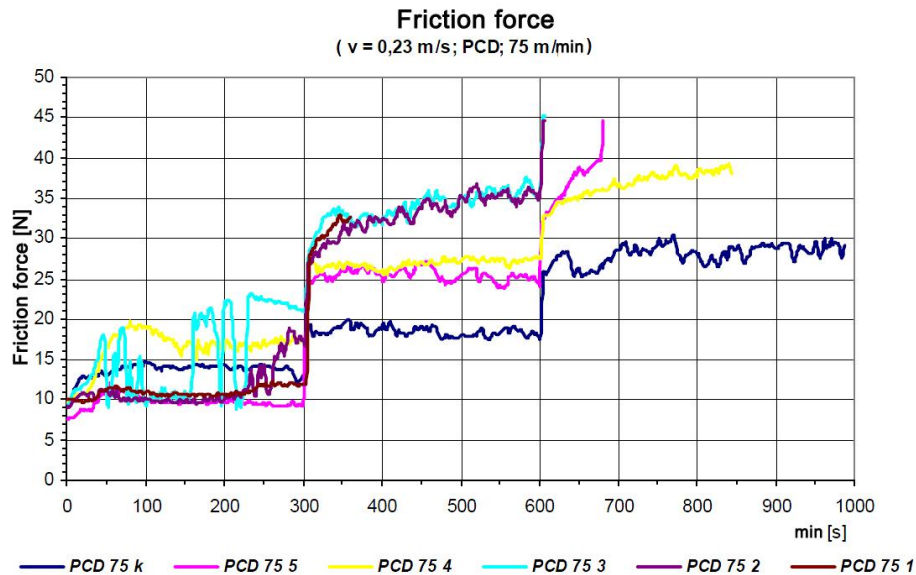


Figure 11. Friction force diagram (between steel/grinded and ceramic surface cut)

Basic difference is comparing with the tests carried out on the surfaces cut at lower cutting speed that the two surfaces seized not at once after imposing the load in the section with the greatest load (150 N). Figure 11. shows the formation of the friction.

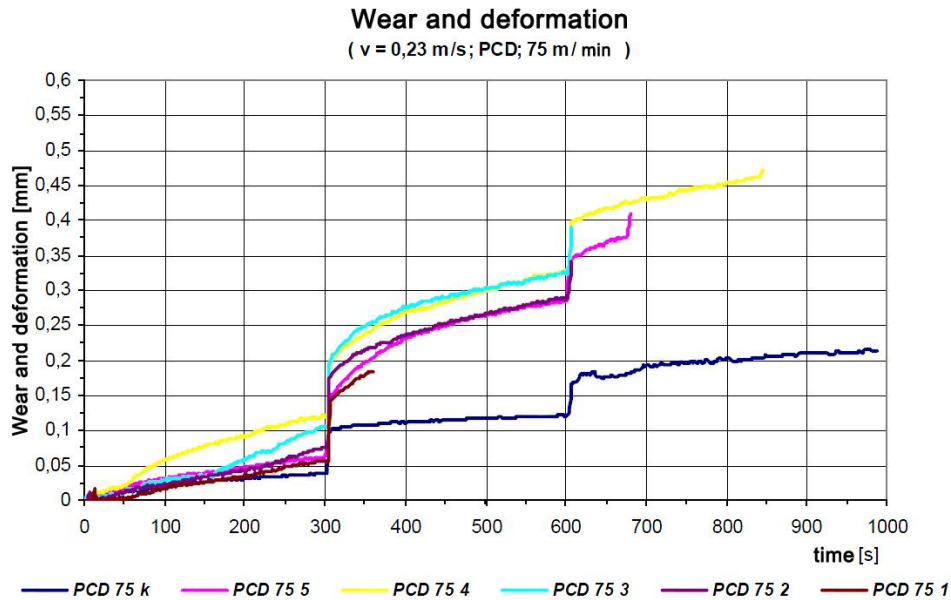


Figure 12. Wear and deformation time-diagram (between steel/grinded and turned ceramic surfaces)

It can be well read from the wear and deformation diagram shown in Figure 12. That these values are lower than those got on the surfaces machined with lower cutting speed. This can be explained thereby that during frictional tests the ceramic surface works off less the steel surfaces.

Figure 13. shows the friction coefficient diagram. The value of the dry friction coefficient between the ceramic surface turned and the steel remains under those measured on grinded surface in this case it occurs already.

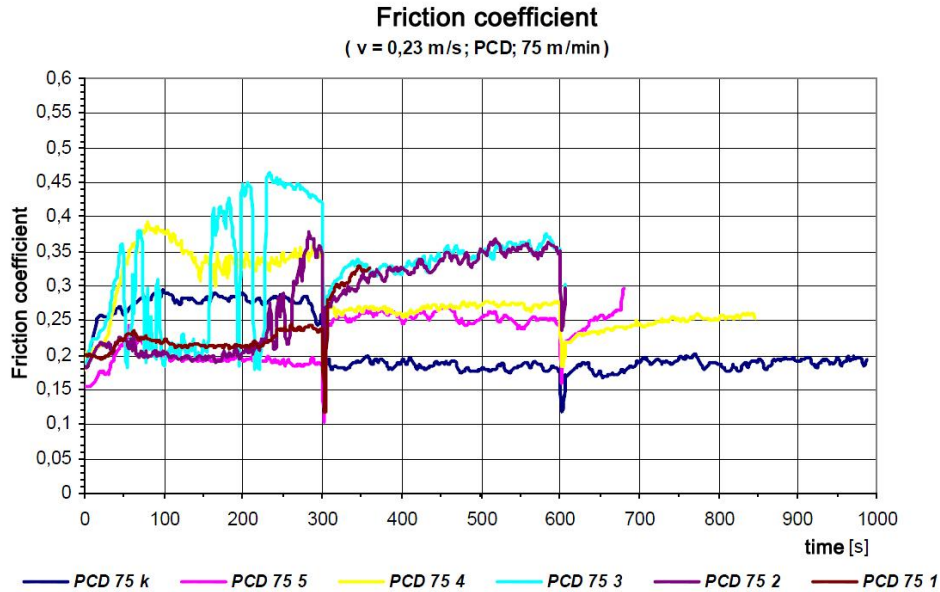


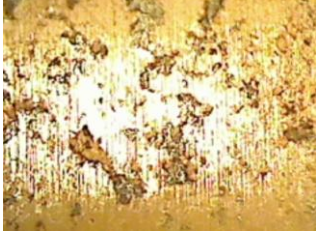
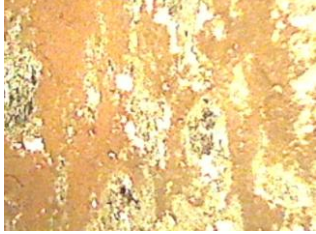
Figure 13. Diagram of friction coefficient (between steel/grinded and ceramic surface cut)

3.4 Microscopic comparison of sliding surfaces

We have made exposures from the dry sliding surfaces of ceramic and steel. The maximum magnification of the microscope was 40x. The pictures show a part of the sliding surface with 40x magnification. We show the sliding test carried out on the surface machined with a given feed rate in Table 2.

It can be seen well on the microscopic exposures of sliding track that at lower speed ($v_c=25 \text{ m/min.}$) the machining is more rough, it resulted greater craters on the ceramic surface. These craters cut the steel surface in a greater extent during sliding test and thus they were filled up with steel faster. After this adhesive connection could develop at certain places between identical materials (steel plate and steel particles stick into craters). This accelerates the seizing process significantly.

Table 2. Microscopic exposures of sliding surfaces (machining parameters: $v_c=25 \text{ m/min.}$, 75 m/min.; $f=0,02 \text{ mm/rev.}$; $a=0,02 \text{ mm}$; test parameters: $v_k=0,23 \text{ m/s}$; $F_n=50 \text{ N}$, 100N; 150N).

tool: PCD	cutting speed 25 m/min	cutting speed 75 m/min
feed rate $f = 0,02 \text{ mm/rev.}$	 ceramic surface 40x	 ceramic surface 40x
	 steel surface 40x	 steel surface 40x

4 CONCLUSIONS

Based on the research program worked out we gave answer to the following unexplained questions: Comparing the arising friction characteristics in dry friction conditions in case of ceramic-steel surface pairs machined with different settings.

We have proved with friction tests (block-on-ring tribological system, St37F grinded steel ($R_a=0,8\text{mm}$) "block" surface, without lubrication, ceramic "ring" specimen) that at high turning cutting speed ($v_c=75\text{ m/min.}$) and at small feed rate ($f=0,01-0,02\text{ mm/rev.}$) the friction resistance is smaller on the ceramic surface. The surface grinded has got smaller dimension but into the great number shell pittings the steel worn particles seat quickly, which transforms the ceramic/steel friction connection into steel/steel characteristic friction, which increases significantly the adhesive component of the friction force.

To evaluate the practical applicability of ceramic surfaces turned and grinded originally, to compare the tribological behaviour have also assembled a laboratory measuring equipment by which we measured the frictional force on steel counter-surface grinded at dry friction condition.

Two main directions can be drawn up to carrying on researches.

- Extending the applicability by changing the technological parameters,
- Technology optimization to be suitable to application-technic standpoints.

The utilization of research results presented in the article indicates advance in the field of machining ceramics spreading better and better in the mechanical engineering practice.

5 REFERENCES

1. Heuer A., Hobbs L. W. (1981): Science and Technology of Zirconia I, *American Ceramic Society, Advances in Ceramics* Vol. 3.
2. Heuer A. H. (1987): Transformation Toughening on ZrO₂-Containing Ceramics. *J. Am. Ceram. Soc.* 70 689-698.
3. Claussen N., Rühle M., Heuer A. (1983); Science and Technology of Zirconia II, *American Ceramic Society, Advances in Ceramics* Vol. 12.
4. Somiya S., Yamamoto N., Yanagida H. (1986): Science and Technology of Zirconia III, *American Ceramic Society, Advances in Ceramics* Vol. 26 A+B.
5. Stevens R. (1986): An Introduction to Zirconia", *publ. by Magnesium Elektron. Deutsche Übersetzung in: Handbuch der Keramik, Deutscher Wirtschaftsdienst*, Kap. 4.2.2.0.
6. Anton van Beek (2006): Advanced Engineering Design. TU Delft, p 87 – 136.
7. Lefánti R., Kalácska G., Oldal I., Petróczki K.(2011):Developing small-aircraft service and re-construction of landing-gear leg support, *Sustainable Construction and Design 2011. Vol. 2. p 99-106*
8. Zsidai L, Kalácska G, Pálinkás I, Ost W (2006): Modular development of dynamic tribological test rig. *Hungarian Agricultural Engineering* 19: pp. 15-18.